Clay Minerals, (2015) **50**, 649–661

Mineralogical and physico-chemical characteristics of Cameroonian smectitic clays after treatment with weakly sulfuric acid

J. R. MACHE[1,2,3,*], P. SIGNING[2], J. A. MBEY[2,4], A. RAZAFITIANAMAHARAVO[4], D. NJOPWOUO[2] AND N. FAGEL[3]

[1] *Mission de Promotion des Matériaux Locaux, B.P. 2396 Yaoundé, Cameroon*
[2] *Laboratoire de Chimie Inorganique Appliquée, Departement de Chimie Inorganique, Université de Yaoundé 1, B.P. 812 Yaoundé, Cameroun*
[3] *UR AGEs Argiles, Géochimie et Environnements sédimentaires, Département de Géologie, Université de Liège, B18, Allée du 6 Août, B-4000 Liège, Belgium*
[4] *Laboratoire Interdisciplinaire des Environnements Continentaux, UMR 7360 CNRS-Université de Lorraine, 15 Avenue du Charmois, B.P. 40. F-54501, Vandœuvre-lès-Nancy Cedex, France*

(*Received 8 April 2014; revised 10 November 2015; Editor: George Christidis*)

ABSTRACT: Smectitic clays from the Sabga and Bana areas, western Cameroon were treated with sulfuric-acid solutions of various concentrations – 0.5, 0.7, 1.0 and 4.0 N – at 80°C for 2 h. The mineralogical, physicochemical and morphological characteristics of the samples treated were analysed using several techniques. The sulfuric acid caused structural modification of the dioctahedral smectite. The accessory minerals such as cristobalite, quartz, feldspars and anatase remained unaltered by the acid attack. The supernatant solutions after acid treatment contain Mg, Ca, K, Na, Si, Al and Fe as a result of partial dissolution of octahedral and tetrahedral cations. The activated clay samples exhibited a smaller cation exchange capacity (CEC) and the specific surface area (SSA) increased with increasing concentration of sulfuric acid, ranging from 65 to 134 m^2/g for the sample from Bana and from 74 to 84 m^2/g for the sample from Sabga. The different SSA values were affected by the relative abundance of smectite and cristobalite ($SiO_2/Al_2O_3 = 2.2$ and 6.5, respectively, from Bana and Sabga). The activated clays from Bana and Sabga displayed interesting physicochemical and textural properties and can be considered as promising adsorbents for the bleaching of vegetable oils.

KEYWORDS: smectite, acid activation, X-ray diffraction, thermal analyses, specific surface area.

INTRODUCTION

Smectites are 2:1 layered aluminosilicate clay minerals which are widely distributed in soils, sediments and prehistoric clay deposits (Karakaya *et al.,* 2011). Due to isomorphic substitution in the tetrahedral and/or octahedral sheets, smectites are characterized by negative structural charges that are compensated by exchangeable cations in the interlayer regions. These cations could be replaced easily by other positively charged species (cations or molecules) (Murray, 1999; Önal & Sarikaya, 2007; Korichi *et al.,* 2009; Ikhtiyarova *et al.,* 2012).

The industrial uses of smectite are related to its reactivity and texture, both of which depend heavily on surface modification. The physico-chemical properties of smectite clays might be modified by pillaring or intercalation treatments, which involve chemical and/or physical restructuring. Microwave or thermal treatment involves modification of the crystal structure

*E-mail: jamache@yahoo.fr
DOI: 10.1180/claymin.2015.050.5.08

and of the chemical composition by temperature. Acid activation (chemical treatment) involves modification of the structure and surface functional groups by forming active sites that enhance adsorption of specific ions or molecules and increase adsorption capacity (Hussin *et al.,* 2011).

Acid activation is a useful method for modifying the catalytic behaviour and enhancing the sorptive properties of clays (Christidis *et al.,* 1997; Steudel *et al.,* 2009; Nguetnkam *et al.,* 2011). Acid treatment is applied commonly to clays used in industry, *e.g.* as catalysts or catalyst supports in alkylation and polymerization reactions (Adams, 1987; Breen, 1991; Rhodes *et al.,* 1991; Rhodes & Brown, 1992, 1993, 1994; Komadel *et al.,* 1997; Mahmoud & Saleh, 1999) and as a component in carbonless copying papers (Fahn & Fenderl, 1983). The most widely used acid-activated clays are probably bleaching earths (Anderson & Williams, 1962; Siddiqui, 1968; Gates *et al.,* 2002; Temuujin *et al.,* 2004), which are capable of removing colour, odour and other impurities from vegetable and animal-edible oils. These practical applications result from physico-chemical activity at the clay surface.

The first step in acid attack during acid treatment is the removal of the exchangeable cations by protons. In the second step, Al, Mg and Fe are leached from octahedral and tetrahedral sheets, but the SiO_4 groups of tetrahedral sheets remain largely intact (Steudel *et al.,* 2009). The increase in the SSA is an important physical change which depends on the dissolution of octahedral sheets. Previous work has shown that acid activation is controlled by treatment time, temperature and acid concentration. The purpose of the present study was to propose and apply acid-activation schemes to local low-quality smectitic clays in developing countries, thereby increasing their added value.

MATERIALS AND METHODS

Materials

Two natural clays with large amounts of dioctahedral smectite associated with kaolinite, quartz, anatase, feldspars and cristobalite (Fig. 1) were used. The clays were collected from Bana in the West Region of Cameroon (BN clay sample) and Sabga in the North West Region of Cameroon (S clay sample) (Mache, 2013; Mache *et al.,* 2013). The <63 μm fractions were separated by wet sieving and decantation and were dried subsequently at 110°C. After drying, the clay samples were crushed to a particle size of <63 μm. The physico-chemical and mineralogical analyses were carried out on the <63 μm fractions.

Acid activation

10 g of each sample was dispersed in 100 mL of 0.5, 0.7, 1.0 and 4.0 N H_2SO_4 (analytical grade, Fischer).

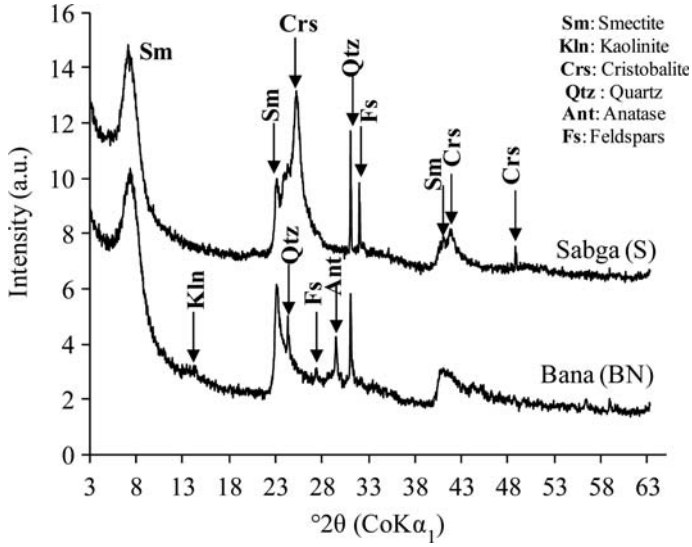

FIG. 1. XRD patterns of the natural clay samples (<63 μm) from Bana (BN) and Sabga (S).

https://doi.org/10.1180/claymin.2015.050.5.08 Published online by Cambridge University Press

The ratio of natural clays (NC) to H_2SO_4 (NC/H_2SO_4 (w/w) varied between 0.2 and 2.0 by mass. The suspension was stirred continuously in a jacketed glass reactor (equipped with water circulation condenser and a thermometer) at 80°C for 2 h. After cooling at room temperature, the suspensions were centrifuged at 3500 rpm and the solid phases were washed several times with pure water (MilliQ ultra filtration) until neutral pH (5% $BaCl_2$ test) and dried at 110°C for 24 h. The samples were then were ground gently with an agate mortar and designated as BN-0.5, BN-0.7, BN-1.0, BN-4.0 (Bana samples) and S-0.5, S-0.7, S-1.0, S-4.0 (Sabga samples), with the suffix (numbers) indicating the concentration of H_2SO_4 solution used during activation. The activated samples were stored in tightly closed plastic bottles for further use.

Characterization

X-ray diffraction (XRD) patterns were obtained from random powder samples using a D8 Advance Bruker diffractometer with CoKα1 radiation (WL = 1.78897), at 35 kV, 45 mA, step scan of 0.036° and step time of 3.0 s. The XRD patterns were recorded in the range 3–63°2θ.

Major elements were determined at CRPG-CNRS (Nancy, France) by emission spectrometry using Inductively Coupled Plasma and Atomic Emission Spectrometry (ICP-AES) after fusion with lithium borate ($LiBO_2$) and dissolution of the glass beads produced in dilute HNO_3. Relative analytical uncertainties were 5% for P_2O_5 and 1–2% for the remaining major elements.

Fourier transform infrared spectroscopy in diffuse reflectance mode was used to investigate the structural changes caused by the acid attack. The IR spectra were recorded using a Bruker IFS 55 spectrometer equipped with an MCT detector. The analysis was performed on KBr pellets containing 15% of activated sample. For each sample, 200 scans with a resolution of 4 cm^{-1} were recorded in the frequency range 4000–600 cm^{-1}. Thermogravimetric-differential thermal analysis (TG-DTA) of the samples was performed using a TA STD 2960, simultaneous DTA-TGA thermal analyzer, at a heating rate of 10°C min^{-1} in air atmosphere.

Changes in particle morphology were observed using a Philips XL30 scanning electron microscope (SEM). The micrographs were obtained using a secondary electron detector at 15 kV accelerating voltage. The samples were deposited on a sample holder with an adhesive carbon foil and coated with gold film.

Nitrogen adsorption-desorption isotherms at 77 K were recorded using a step-by-step automatic home-built device. The SSA values were determined from adsorption data by applying the Brunauer-Emmet-Teller (BET – Brunauer *et al.,* 1940) equation. Micropore and non-microporous surface areas were assessed using the t-plot method (De Boer *et al.,* 1966). Pore-size distributions were calculated on the desorption branch using the Barrett-Joyner-Halenda method (BJH, Barrett *et al.,* 1951) assuming slit-like pore shape.

The particle-size distribution (PSD) of the samples (0.02–2000 µm range) was determined using a Malvern Instruments Mastersizer-2000 device. In order to avoid flocculation, the suspensions were dispersed by ultrasound for 5 min using a Fisher Scientific FB15047 Ultrasound device. They were then placed in the small-volume compartment, stirred at 2000 rpm and sonicated before measurement. The measuring ranges were 0.02–2000 µm, and each result obtained was the average of four measurements.

The cation exchange capacity (CEC) was measured using hexaminecobalt(III)chloride [$Co(NH_3)_6Cl_3$] as exchangeable ions. The amount of hexaminecobalt (III) fixed by the solid phase was determined by colorimetric measurement at 472 nm using UV-vis spectroscopy. The displaced cations were determined by atomic absorption spectrometry (Perkin-Elmer 1100B). The pH of the clays was measured using a 905 Titrando pH-meter from 'Ω Metrohm' following stirring of a 1:5 sample/milli Q water suspension for 30 min and standing for 1 h.

Capillary ion analysis (CIA) and Atomic absorption spectrometry (Model Nov AA 300, Analytik Jena, Germany) were used to determine the concentrations of Ca^{2+}, Na^+, K^+, Mg^{2+} and Si, Al, Cu, Co, Cr, Fe, Ni, Pb, Sr, Ti, V and Zn, respectively, in the supernatant solutions after acid treatment.

RESULTS AND DISCUSSION

Structural modification under acid treatment

The XRD patterns of activated clays with the H_2SO_4 solutions are presented in Fig. 2. Activation has affected mainly the 001 basal reflection of smectite; its intensity decreased significantly with increase in acid concentration. The effect of acid concentration on the smectite structure is similar in both clay samples (Fig. 2) and in agreement with previous work (Christidis *et al.,* 1997; Srasra *et al.,* 1989; Nguetnkam *et al.,* 2011). Acid-activated samples displayed a slight increase in the

https://doi.org/10.1180/claymin.2015.050.5.08 Published online by Cambridge University Press

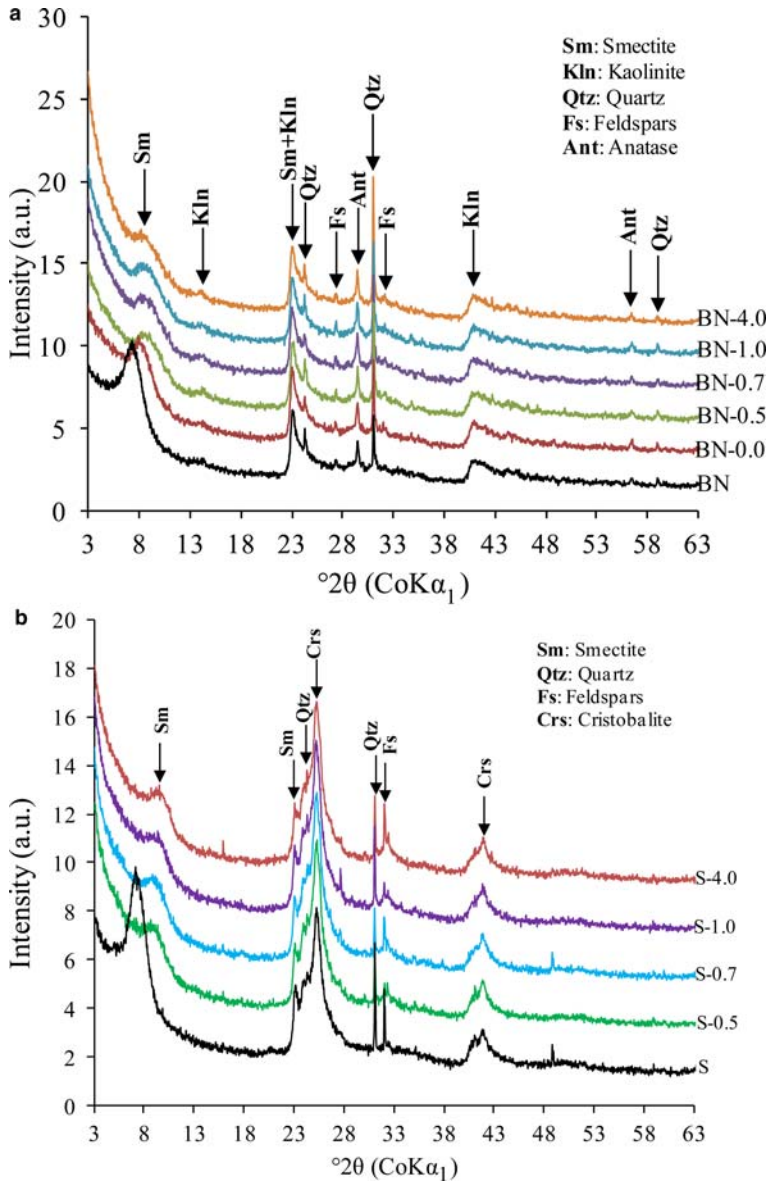

FIG. 2. XRD patterns of the acid-activated clay samples: (a) Bana; (b) Sabga.

background between 21 and 35°2θ which is attributed to the deposition of amorphous SiO_2 from the acid attack on the octahedral sheet and the exposure of the tetrahedral sheet (Christidis *et al.,* 1997; Nguetnkam *et al.,* 2011). In the XRD patterns of the acid-treated clays from Bana (Fig. 2a), the d_{001} reflection of kaolinite remains unchanged suggesting that acid activation up to 4 N does not affect its structure. The (11 l) diffraction maxima are present for the whole range of concentrations used in this work, indicating that clay layers are not fully dissolved during acid treatment. The structural changes caused by acid activation are observed through the shift of the d_{001} spacing towards lower values with decreasing intensity and smoothing of the main smectite peaks in the XRD patterns. During the acid attack, the protons penetrate into the smectite layer and attack the structural OH groups (Bergaya *et al.,* 2006). The resulting dehydroxylation is followed by

https://doi.org/10.1180/claymin.2015.050.5.08 Published online by Cambridge University Press

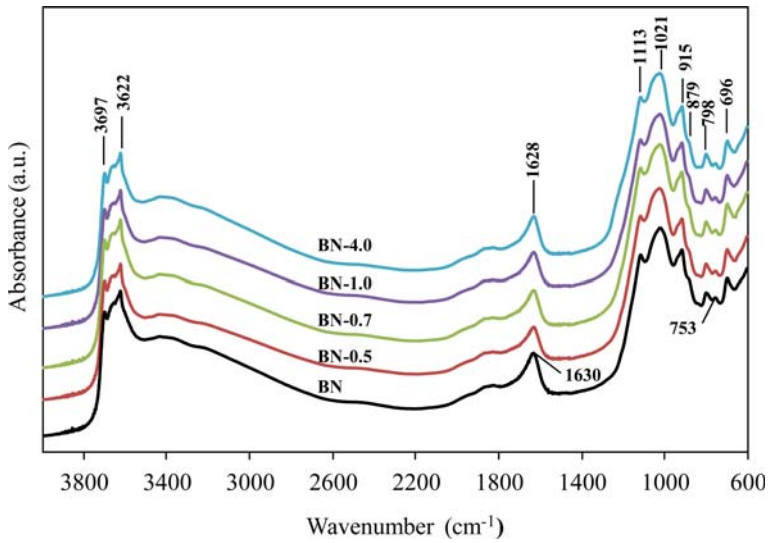

FIG. 3. FTIR spectra of the Bana smectite and the products of acid activation, using various H_2SO_4 concentrations.

successive release of the octahedral Mg and tetrahedral Al (Bergaya *et al.,* 2006). The diffraction maxima of the associated minerals (quartz, cristobalite and feldspars) were still detected after activation because they dissolved more slowly and no new additional phases were observed in the activation products.

The FTIR spectra of untreated and treated clays are shown in Figs 3 and 4. The bands at 3697 cm^{-1} and 3622 cm^{-1}, corresponding to stretching vibrations of Al-Al-OH in kaolinite or smectite, are obvious in the BN-treated samples, suggesting that these two bands are less sensitive during treatment with acid of weak concentration (Christidis *et al.,* 1997).

The band at 3636 cm^{-1}, highlighted in Fig. 4, corresponds to Al-Al-OH stretching of smectite (Madejová *et al.,* 1994) and remains unaffected by the increase in acid concentration. This is attributed to the small acid concentrations used to activate the

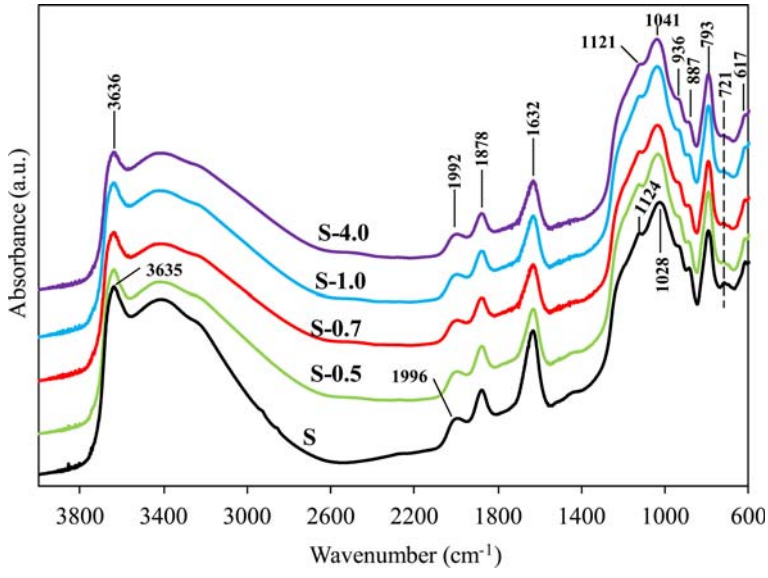

FIG. 4. FTIR spectra of the Sabga smectite and the products of acid activation, using various H_2SO_4 concentrations.

https://doi.org/10.1180/claymin.2015.050.5.08 Published online by Cambridge University Press

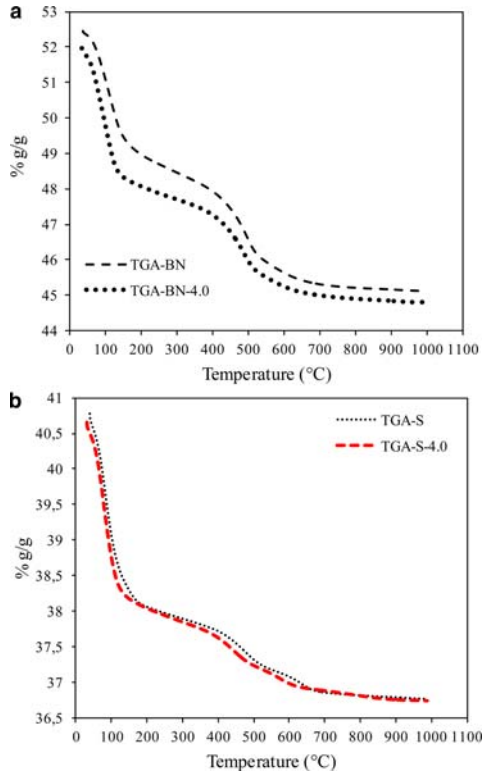

FIG. 5. (a) TGA curves of treated and untreated sample 'BN'; (b) TGA curves of treated and untreated sample 'S'.

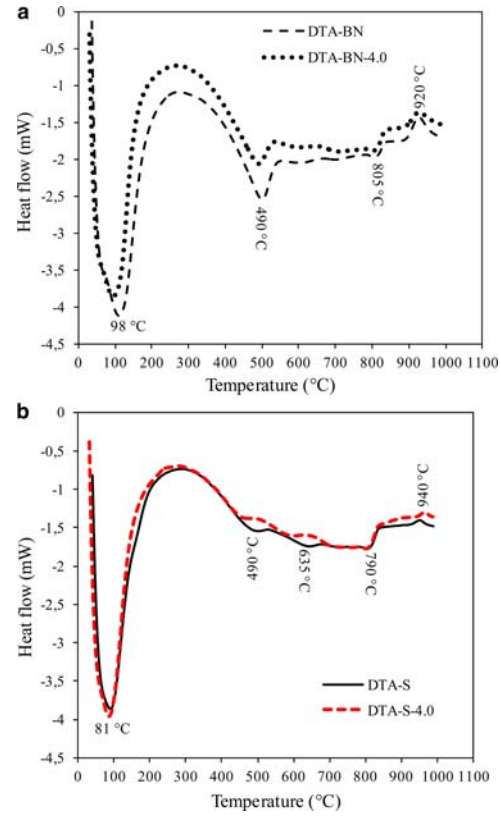

FIG. 6. (a) DTA curves of treated and untreated sample 'BN'; (b) DTA curves of treated and untreated sample 'S'.

clays compared with similar studies which used more concentrated acids. The bands at 1628–1632 cm^{-1} are attributed to the bending vibration of adsorbed water for both samples (Figs 3, 4). The broad bands at 1021 cm^{-1} and 1041 cm^{-1} in the spectra of BN and S samples, respectively, are attributed to the Si–O stretching vibration (in-plane). However, the bands at 798 cm^{-1} and 793 cm^{-1} are due to cristobalite and the amorphous silica which formed during the acid treatment (Figs 3, 4) (Madejová, 2003; Nguetnkam *et al.,* 2011). The weak bands at 1113 cm^{-1} and 1121 cm^{-1} observed in the BN and S spectra, respectively, are assigned to the Si–O stretching vibration (out-of-plane). The intensity of Al-Al-OH bending bands at 915 cm^{-1} remained constant after treatment with various acid concentrations, suggesting that this band is associated not only with Al-Al-OH vibrations of smectite but also with the vibrations of kaolinite (Madejová, 2003). This observation is in agreement with the XRD results, which showed that the 001 reflection of kaolinite and the residual smectite are still visible after acid activation up to 4.0 N. The band at 887 cm^{-1}, corresponding to Al-Fe-OH vibration in the spectra of S samples remained unchanged (Fig. 4), suggesting that the acid treatment does not affect structural iron. The strong band at 793 cm^{-1} associated with cristobalite observed in Sabga clay, persists after treatment, in accordance with the XRD results. Furthermore, the band at 696 cm^{-1} in BN samples indicates the presence of quartz. The weak absorption band at 617 cm^{-1} observed in S samples can be identified as the perpendicular vibration of the octahedral cations (R–O–Si, R = Al, Mg, Fe). The IR spectra of the untreated and treated clay samples from Sabga also revealed the presence of SiO_2 impurities. Finally, the bands at 1878 and 1992 cm^{-1}, which could be ascribed to quartz and cristobalite, were observed as impurities in the XRD patterns (Gates *et al.,* 2002).

The effects of acid activation on the thermal behaviour of the two smectite-based clays (Figs 5, 6) are summarized as follows. The loss of adsorbed and

https://doi.org/10.1180/claymin.2015.050.5.08 Published online by Cambridge University Press

TABLE 1. Major elements (wt.%) of the natural samples and samples treated with 4 N sulfuric acid.

Major elements (wt.%)	BN	BN-4.0	S	S-4.0
SiO_2	50.94	54.58	73.39	75.57
Al_2O_3	22.39	20.52	11.43	11.00
Fe_2O_3	5.52	4.93	4.83	4.37
MnO	0.01	0.00	0.01	0.00
MgO	1.85	1.76	0.35	0.09
CaO	0.05	bdl	0.55	0.11
Na_2O	0.02	0.02	0.26	0.25
K_2O	0.70	0.71	0.48	0.40
TiO_2	2.31	2.45	0.17	0.18
P_2O_5	0.26	0.14	0.03	bdl
L.O.I.	16.15	15.26	9.30	8.49
Total	100.20	100.38	100.79	bdl
SiO_2/Al_2O_3	2.28	2.66	6.42	6.87

bdl: below detection limits.

interlayer water is still observed in the acid-treated samples at ~100°C. The area of the dehydration (endothermic peaks at ~81°C) remains essentially unchanged for Sabga sample (S) treated at 4 N (Fig. 5b). The Bana clay sample (BN) showed a change in the area of the endothermic peak when the clay was treated with 4 N acid, however (Fig. 5a). Total weight losses of 7.3% and 5.6% for untreated and treated BN clays, respectively, were observed (Fig. 5a). In the S clay the weight losses of the original and the activated samples were essentially identical (4% and 3.9%, respectively, Fig. 5b). The intensity of the main dehydroxylation peak of the BN sample at ~490°C decreased after activation with 4 N sulfuric acid (Fig. 6a). In the S sample two endothermic peaks were observed at 490 and 635°C and were broader. Moreover, they were shifted to lower temperatures (435 and 560°C, respectively, and are associated with smaller weight losses (Figs 5b, 6b). The exothermic peak observed at ~920°C in the untreated sample due to recrystallization of the smectite structure became weaker after activation with 4 N H_2SO_4 suggesting that activation with H_2SO_4 affects the crystal order of the smectite phase in the BN samples. The weak changes observed during acid treatment of sample S confirmed that the acid concentrations used in the present study do not destroy the structure of smectite completely (see XRD patterns in Fig. 2b).

The number of defects or disorders in the clay minerals in both clay samples increased gradually with increasing acid concentration. This increase affects some physico-chemical properties of the clays.

TABLE 2. Cations (mg/L) leached after acid treatment (1.0 and 4.0 N).

Cations leached (mg/L)	BN	BN-1.0	BN-4.0	S	S-1.0	S-4.0
Ca	0.21	>120	>300	2.62	328.85	>300
Mg	0.05	107.95	208.49	1.09	89.47	>200
K	0.75	>200	>500	1.80	>200	>500
Na	nd	nd	nd	1.51	225.76	432.00
Al	0.94	1195	2176	22.43	504	647
Si	33.33	193	774	131	238	470
Fe	0.12	392	904	15.70	464	482
Ti	0.00	0.00	0.00	0.00	0.00	0.00
Cu	nd	nd	nd	0.02	0.25	0.26
Co	0.00	0.34	0.60	0.01	0.27	0.46
Cr	nd	nd	nd	0.00	0.03	0.01
Ni	nd	nd	nd	0.00	0.24	0.54
Pb	0.00	0.53	0.84	0.01	0.49	0.76
Sr	0.00	0.04	0.05	0.00	0.26	0.14
V	0.35	3.98	6.00	0.00	0.00	0.00
Zn	0.01	1.36	1.86	0.14	6.58	7.99

nd: not determined.

https://doi.org/10.1180/claymin.2015.050.5.08 Published online by Cambridge University Press

Table 3. CEC and pH of the natural and acid-activated samples.

Sample	CEC[1] (mmol/g)	CEC[2] (mmol/g)	pH
BN	56	60	4.2
BN-0.5	53	49	3.4
BN-0.7	52	50	3.2
BN-1.0	52	46	3.2
BN-4.0	46	28	3.6
S	38	36	5.8
S-0.5	27	15	3.9
S-0.7	26	14	3.7
S-1.0	25	12	3.6
S-4.0	25	12	3.2

[1]derived from the measurement of cobaltihexamine concentrations by UV-Vis spectroscopy.
[2]derived from chemical analysis of displaced cations.

Chemical evolution of smectite under acid treatment

The major-element analysis of the smectitic clays performed using ICP-AES provided evidence of changes in the samples' compositions after acid treatment (Table 1). By increasing the sulfuric acid concentration from 0.0 to 4.0 N in both clay samples, reduction in the CaO content was observed indicating that the Ca^{2+} cations were replaced by H^+ protons and/or cations leached from octahedral sheet. In view of this net reduction during the treatment, Ca^{2+} cations were probably the exchangeable cation form in both samples. With advancing acid activation, the percentages of Na_2O and K_2O remained almost unchanged while that of SiO_2 increased. The same behaviour was observed in the ratio of $SiO_2/(Al_2O_3 + Fe_2O_3 + MgO)$ which increased in both samples up to 4.0 N.

The unchanged percentages of Na_2O and K_2O are probably due to the presence of stable Na or K-feldspars, in agreement with the XRD results. The increase in SiO_2 content during activation was residual and due to the leaching of octahedral cations. Indeed, during activation, partial leaching of the octahedral cations took place and this is indicated by the decrease in the MgO, Fe_2O_3 and Al_2O_3 contents. A significant proportion of the octahedral cations was retained, following acid activation by 4.0 N H_2SO_4, suggesting that the layered structure of smectite in the two samples was only partially destroyed. The different amounts of the octahedral cation oxides leached from the samples (Mg, Fe and Al) indicate the possible presence of the cations both in readily soluble or exchangeable forms (*e.g.* Mg) and in minerals that are more resistant to acid attack (*e.g.* feldspars). The loss on ignition at 1100°C of the activated samples decreased with increasing acid concentration, probably due to leaching of octahedral cations linked to OH-groups (Al-Al-OH, Al-Fe-OH

Table 4. Surface properties resulting from N_2 adsorption isotherms of the natural and activated clays.

Sample	Specific surface area S_{BET} (m^2/g) BET method[1]	Micropore surface area (m^2/g) t-plot method (de Boer *et al.*, 1966)	Non-micropore surface area (m^2/g) t-plot method (de Boer *et al.*, 1966)
BN	64.8	28.2	40.8
BN-0.5	76.0	29.5	51.0
BN-0.7	82.6	30.4	56.0
BN-1.0	92.4	32.2	64.3
BN-4.0	134.3	27.6	110.1
S	74.0	18.0	58.7
S-0.5	77.7	19.6	60.7
S-0.7	78.8	19.7	61.6
S-1.0	79.2	21.1	60.9
S-4.0	83.7	26.3	60.6

[1]The error in determination of S_{BET} was ±3%.

https://doi.org/10.1180/claymin.2015.050.5.08 Published online by Cambridge University Press

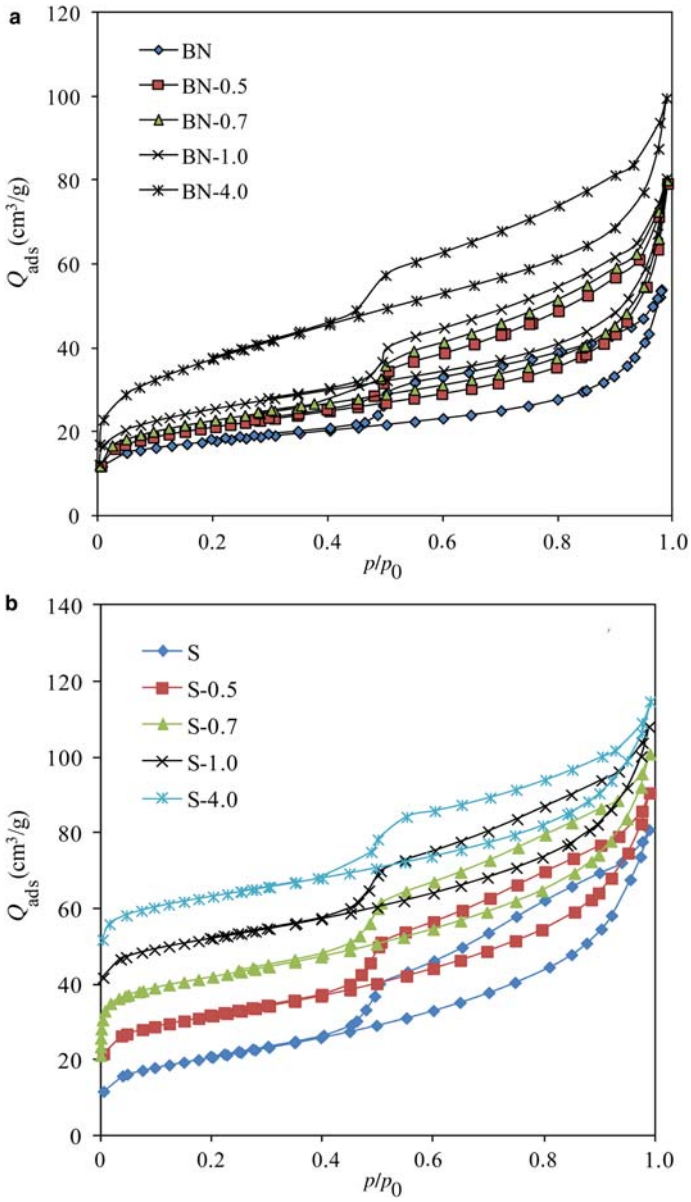

FIG. 7. N_2 adsorption/desorption isotherms of the natural and acid-activated clays at 77 K: (a) samples from Bana; (b) samples from Sabga.

and Al-Mg-OH) from the smectite structure, in accordance with previous studies (Gates *et al.,* 2002; Amari *et al.,* 2010).

The effect of acid concentration on the leaching of the cations from the two clay samples during acid treatment is shown in Table 2. The amount of Ca^{2+}, Mg^{2+}, Na^+ and K^+ removed by acid treatment increased with increasing acid concentration up to 4 N. The Ca^{2+}, Na^+ and K^+ removed by acid treatment corresponded to the exchangeable cations located in the interlayer, so that they are released under mild conditions. The amount of Al, Si and Fe leached during acid attack increased with acid concentration (Table 2). In contrast, no Ti was

https://doi.org/10.1180/claymin.2015.050.5.08 Published online by Cambridge University Press

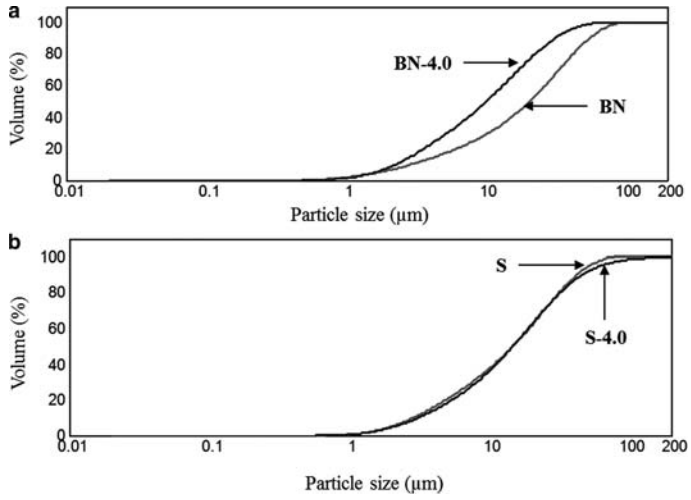

FIG. 8. Particle-size distribution of the untreated and acid-treated samples: (a) samples from Bana: natural (BN) and treated (BN-4.0); (b) samples from Sabga: natural (S) and treated (S-4.0).

determined in the filtrates, in agreement with the XRD patterns which showed that anatase is resistant to acid attack.

The variations in the CEC and pH values with H_2SO_4 concentration are listed in Table 3. The CEC values display similar trends in both materials and they decrease continuously with increasing degree of activation in the two clay samples. This progressive decrease in CEC values upon treatment with sulfuric acid can be explained in terms of the leaching of the octahedral sheet. Leaching of the octahedral cations (Mg^{2+}, Fe^{2+}) results in the reduction of negative layer charge and therefore of the CEC) (Breen *et al.,* 1995; Falaras *et al.,* 1999). Finally, the pH values of activated clays are small compared to those of initial clays, due to the replacement of the interlayer cations by protons (H^+) during the treatment, in agreement with similar work on industrial adsorbents and activated clays (Nguetnkam *et al.,* 2011).

Textural properties, particle-size distribution and microstructure

The BN and S natural clays have SSA values of 65 and 74 m^2/g, respectively. These values are within the typical surface-area values for smectite (50–120 m^2/g, Morgan *et al.,* 1985; van Olphen & Fripiat, 1979), and confirm that the two clays consist mainly of very small particles of smectite (Christidis *et al*., 1997). The SSA values of both clays increased continuously with acid concentration during activation (Table 4). The SSA of the Bana clay increased more quickly than did that of the Sabga clay during acid treatment (134 and 84 m^2/g, respectively, after treatment with 4 N acid). The SSA of the activated product from Bana is about twice as great as that of the natural clay after activation with 4 N acid. The small SSA of the Sabga bentonite is due to the abundance of SiO_2 polymorphs, especially cristobalite. The effect of treatment with sulfuric acid is slightly greater on the BN samples, resulting in a decrease in the microporosity and increase in non-micropore surface areas. For Sabga samples, however, acid treatment resulted in a significant increase in non-micropore surface areas compared to the micropore surfaces (Table 4). In addition, the changes in SSA, depending on the acid concentration, are greater for sample BN than for sample S. Generally, stronger acid enhances the destruction of the clay structure thereby increasing the SSA.

The N_2 adsorption/desorption isotherms of natural and acid-treated clay samples obtained at ~77 K are shown in Fig. 7. The adsorption capacity (Q_{ads}) increases continuously with increasing H_2SO_4 concentration. This can be explained in terms of increasing porosity in the samples. All the isotherms are similar to Type II according to the classification of Brunauer *et al.* (1940), characteristic of mesoporous solids which also contain some micropores. The overlapping of the adsorption-desorption isotherms over the interval $0 < p/p_0 < 0.35$ shows that the multimolecular and monomolecular adsorption is reversible.

https://doi.org/10.1180/claymin.2015.050.5.08 Published online by Cambridge University Press

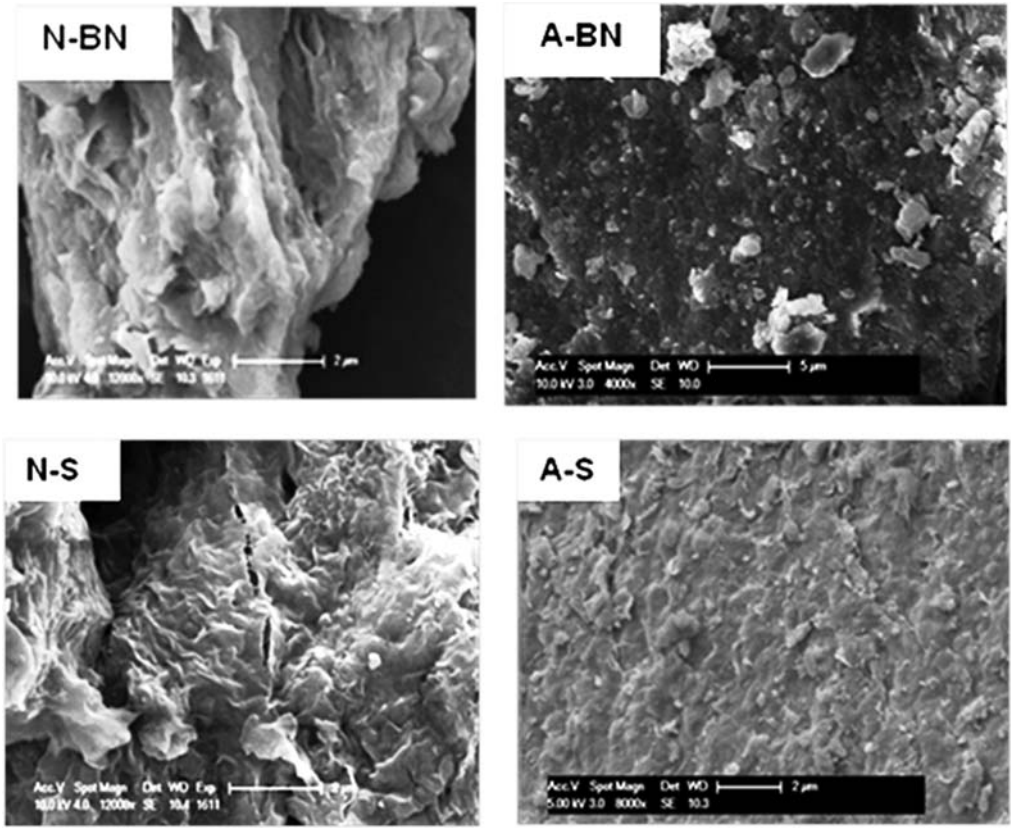

FIG. 9. SEM images of natural and acid-activated products using 4.0 N H_2SO_4:N-BN and N-S (samples from Bana and Sabga, respectively); A-BN and A-S (acid-activated samples from Bana and Sabga, respectively).

The particle-size distribution of the samples is shown in Fig. 8. The BN sample activated with 4.0 N H_2SO_4 exhibits an increased proportion of particle sizes between 2.2 μm and 45 μm (Fig. 8a). In contrast, the particle size of sample S was not modified significantly by acid treatment (Fig. 8b). The increase in the SSA of the acid-treated samples may also be linked with an increase in the proportion of coarser particles which dissolved during acid attack.

Scanning electron microscopy was used to confirm the morphological changes between natural and activated clays. The wavy subhedral and honeycomb textures of smectite in the untreated samples (N-BN and N-S) are shown in Fig. 9. After treatment with sulfuric acid up to 4.0 N, the wavy subhedral and honeycomb textures of smectite were replaced by flat flakes (see A-BN and A-S in Fig. 8). These observations are in agreement with the XRD results from the structural changes of smectite. The flat black flakes observed in treated BN samples (A-BN) probably belong to amorphous material (SiO_2) produced during acid activation.

CONCLUSIONS

The effect of the acid activation on the physicochemical and mineralogical properties of smectite was evaluated on natural clays from Cameroon. Acid treatment of these clays containing accessory quartz, cristobalite, anatase and feldspars led to the following conclusions:

(1) The XRD results show a progressive decrease in intensity and partial disappearance of basal reflections of smectite. The reflections of non-clay minerals present in both samples remained essentially unchanged though the relative intensity of quartz reflections increased. The FTIR spectra confirmed that the sulfuric-acid concentrations used in the present

https://doi.org/10.1180/claymin.2015.050.5.08 Published online by Cambridge University Press

study do not affect the structure of clay minerals significantly in either sample.

(2) Increase in H_2SO_4 concentration up to 4 N causes the release of cations (Ca, K, Mg, Na, Al, Fe and Si) from the structure of smectite. Titanium was not leached during acid treatment, indicating that anatase was not dissolved. The tetrahedral cations were, in general, the most resistant to acid attack, followed by the octahedral cations; exchangeable cations are the most mobile.

(3) The SSA of acid-activated samples increased with increasing acid concentration, up to 134 m^2/g and 84 m^2/g for BN and S clay samples respectively, after activation with 4 N acid. The changes in SSA are associated with changes in the smectite structure during treatment. This method can be useful for manufacturing active and porous materials with large SSA values which can be used for bleaching of edible oil as well as adsorbents.

ACKNOWLEDGEMENTS

The present study was supported by No. O.ACRDGEN 01-17-F-0060- Federal grant for research in the 'Laboratoire Environnement et Minéralurgie' (Nancy, France), financed by the University of Liege. The authors thank Thomas Fabien for his help with the analytical equipment and Professor Agwara Moise Ondoh of the University of Yaoundé for editing the English in the manuscript.

REFERENCES

Adams J.M. (1987) Synthetic organic chemistry using pillared, cation-exchanged and acid-treated montmorillonite catalysts – a review. *Applied Clay Science*, **2**, 309–342.

Amari A., Chlendi M., Gannouni A. & Bellagi A. (2010) Optimised activation of bentonite for toluene adsorption. *Applied Clay Science*, **47**, 457–461.

Anderson A.J.C. & Williams P.N. (1962) *Refining of Oils and Fats for Edible Purposes.* Pergamon, New York.

Barrett E.P., Joyner L.G. & Halenda P.P. (1951) The determination of pore volume and area distributions in porous substances. I. Computation from nitrogen isotherms. *Journal of the American Chemical Society*, **73**, 373–380.

Bergaya F., Theng B.K.G. & Lagaly G. (2006) *Handbook of Clay Science.* Developments in Clay Science, **1**, Elsevier, Amsterdam.

Breen C. (1991) Thermogravimetric study of the desorption of cyclohexylamine and pyridine from an acid-treated Wyoming bentonite. *Clay Minerals*, **26**, 473–486.

Breen C., Madejová J. & Komadel P. (1995) Characterization of moderately acid-treated, size fractionated montmorillonites using IR and MAS NMR spectroscopy and thermal analysis. *Journal of Materials Chemistry*, **5**, 469–474.

Brunauer S., Deming L.S., Deming D.M. & Teller E. (1940) On a theory of the van der Waals adsorption on gases. *Journal of the American Chemical Society*, **62**, 1723–1732.

Christidis G.E., Scott P.W. & Dunham A.C. (1997) Acid activation and bleaching capacity of bentonites from the Island of Milos and Chios, Aegean, Greece. *Applied Clay Science*, **12**, 329–347.

De Boer J.H., Lippens B.C., Linsen B.G., Brokhoff J.C.P., Van DerHeuvel A. & Osinga T.J. (1966) The t-cuve of multimolecular N_2 adsorption. *Journal of Colloid and Interface Science*, **21**, 405–414.

Fahn R. & Fenderl K. (1983) Reaction products of organic dye molecules with acid-treated montmorillonites. *Clay Minerals*, **18**, 447–458.

Falaras P., Kovanis I., Lezou F. & Seiragakis G. (1999) Cotton oil bleaching by acid-activated montmorillonite. *Clay Minerals*, **34**, 221–232.

Gates W.P., Anderson J.S., Raven M.D. & Churchman G.J. (2002) Mineralogy of a bentonite from Miles, Queensland, Australia and characterization of its acid activation products. *Applied Clay Science*, **20**, 189–197.

Hussin F., Aroua M.K. & Wan Daud W.M.A. (2011) Textural characteristic, surface chemistry and activation of bleaching earth: A review. *Chemical Engineering Journal*, **170**, 90–106.

Ikhtiyarova G.A., Özcan A.S., Gök Ö. & Özcan A. (2012) Characterization of natural- and organo-bentonite by XRD, SEM, FT-IR and thermal analysis techniques and its adsorption behavior in aqueous solutions. *Clay Minerals*, **47**, 31–44.

Karakaya M.Ç., Karakaya N. & Küpeli Ş. (2011) Mineralogical and geochemical properties of the Na- and Ca-bentonite of Ordu (NE Turkey). *Clays and Clay Minerals*, **59**, 75–94.

Komadel P., Janek M., Madejová J., Weekes A. & Breen C. (1997) Acidity and catalyitic activity of mildly acid-treated Mg-rich montmorillonite and hectorite. *Journal of the Chemical Society, Faraday Transactions*, **93**, 4207–4210.

Korichi S., Elias A. & Mefti A. (2009) Characterization of smectite after acid activation with microwave irradiation. *Applied Clay Science*, **42**, 432–438.

Mache J.R. (2013) *Minéralogie et propriétés physico-chimiques des smectites de Bana et Sabga (Cameroun): utilisation dans la décoloration d'une huile végétale alimentaire.* Thèse de Doctorat en Sciences de l'Université de Liège, Belgium, 145 pp.

Mache J.R., Signing P., Njoya A., Kunyukubundo F., Mbey J.A., Njopwouo D. & Fagel N. (2013) Smectite clay from the Sabga deposit (Cameroon): mineralogical and physicochemical properties. *Clay Minerals*, **48**, 499–512.

Madejová J. (2003) FTIR techniques in clay mineral studies. *Vibration Spectroscopy*, **31**, 1–10.

https://doi.org/10.1180/claymin.2015.050.5.08 Published online by Cambridge University Press

Madejová J., Komdel P. & Čičel B. (1994) Infrared study of octahedral site populations in smectites. *Clay Minerals*, **29**, 319–326.

Mahmoud S. & Saleh S. (1999) Effect of acid activation on the de-tert-butylation activity of some Jordanian clays. *Clays and Clay Minerals*, **47**, 481–486.

Morgan D.A., Shaw D.B., Sidebottom M.J., Soon T.C. & Taylor R.S. (1985) The function of bleaching earths in the processing of palm, palm kernel and coconut oils. *Journal of the American Oil Chemists' Society*, **62**, 292–299.

Murray H.H. (1999) Applied clay mineralogy today and tomorrow. *Clay Minerals*, **34**, 39–49.

Nguetnkam J.P., Kamga R., Villiéras F., Ekodeck G.E., Razafitianamaharavo A. & Yvon J. (2011) Alteration of Cameroonian clays under acid treatment. Comparison with industrial adsorbents. *Applied Clay Science*, **52**, 122–132.

Önal M. & Sarikaya Y. (2007) Preparation and characterization of acid-activated bentonite powders. *Powder Technology*, **172**, 14–18.

Rhodes C.N. & Brown D.R. (1992) Structural characterisation and optimisation of acid-treated montmorillonite and high porosity silica supports for $ZnCl_2$ alkylation catalysts. *Journal of the Chemical Society, Faraday Transactions*, **88**, 2269–2274.

Rhodes C.N. & Brown D.R. (1993) Surface properties and porosities of silica and acid-treated montmorillonite catalyst supports: influence on activities of supported $ZnCl_2$ catalysts. *Journal of the Chemical Society, Faraday Transactions*, **89**, 1387–1391.

Rhodes C.N. & Brown D.R. (1994) Catalytic activity of acid-treated montmorillonite in polar and non-polar reaction media. *Catalysis Letters*, **24**, 285–291.

Rhodes C.N., Franks M., Parkes G.M.B. & Brown D.R. (1991) The effect of acid treatment on the activity of clay supports for ZnCl2 alkylation catalysts. *Journal of the Chemical Society, Chemical Communications*, 804–807.

Srasra E., Bergaya F., Van Damme H. & Ariguib N.K. (1989) Surface properties of activated bentonite: decolorization of rape seed oil. *Applied Clay Science*, **4**, 411–421.

Siddiqui M.K.H. (1968) *Bleaching Earths.* Pergamon, Oxford, UK, 86 pp.

Steudel A., Batenburg L.F., Fischer H.R., Weidler P.G. & Emmerich K. (2009) Alteration of swelling clay minerals by acid activation. *Applied Clay Science*, **44**, 105–115.

Temuujin J., Jadambaa Ts., Burmaa G., Erdenechimeg Sh., Amarsanaa J. & MacKenzie K.J.D. (2004) Characterisation of acid activated montmorillonite clay from Tuulant (Mongolia). *Ceramics International*, **30**, 251–255.

Van Olphen H. & Fripiat J.J. (1979) *Data Handbook for Clay Materials and Other Non-Metallic Minerals.* Pergamon Press, Oxford, UK.

https://doi.org/10.1180/claymin.2015.050.5.08 Published online by Cambridge University Press